ChemComm

CrossMark
← click for updates

Observation of a reversible isomorphous phase transition and an interplay of "σ-holes" and "π-holes" in Fmoc-Leu-ψ[CH₂-NCS]†

Rumpa Pal,[a] Govindappa Nagendra,[b] M. Samarasimhareddy,[b] Vommina V. Sureshbabu[b] and Tayur N. Guru Row*[a]

Fmoc-Leu-ψ[CH₂NCS] undergoes a reversible isomorphous phase transition upon cooling. The crystal structure at 100 K displays a short N═C═S···N═C═S intermolecular interaction, which has been characterized based on experimental charge density analysis, as a stabilizing interaction with both σ-holes and π-holes acting cooperatively.

In recent years, it has been demonstrated that bioactive peptides with unnatural bonds in place of peptide bonds show enhanced pharmacokinetic properties.[1,2] In this context, organic isothiocyanates, which are versatile synthetic intermediates, have been subjected to extensive structure–property correlation studies.[3] Though isothiocyanates are known to readily participate in nucleophilic addition and cycloaddition reactions owing to their high electrophilicity, quantitative analysis of interactions involving isothiocyanate moieties in crystal structures have received very little attention. Interestingly, crystal structures of several thiocyanates (–SCN), isomers of isothiocyanates (–NCS), have been explored during the early days of experimental and theoretical charge density analyses[4–6] to understand the features of non-covalent interactions involving the –SCN moiety.
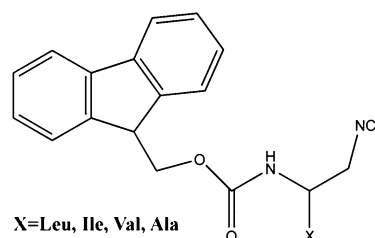
Some of the well-studied non-covalent interactions in biological molecules are hydrogen bonding, π–π stacking, and cation–π interactions, while anion–π and more generally the lone pair–π interactions and halogen bonding are the new entrants. Halogen bonding is a subset of σ hole bonding which explains the anomaly of an electronegative halogen interacting attractively with a negative site on the same or another molecular system. The concept of σ-holes was invoked to describe the extension of a covalent bond of an atom (groups IV–VII of the periodic table) and their counterparts, π-holes,

describe the region of positive electrostatic potential perpendicular to a portion of the molecular framework.[7,8] Both σ-holes and π-holes are highly directional and the structural studies of N_β Fmoc-protected β amino alkyl isothiocyanates {Fmoc-X-ψ[CH₂NCS] (X = Leu, Ile, Val and Ala)} provide a unique opportunity to investigate the features of the electrostatic potentials associated with the isothiocyanate moiety. Though computational studies on π-hole containing molecules have been reported in the literature elucidating the nature of π-hole bonding,[9,10] experimental results have not been studied in detail to the best of our knowledge. However, it may be mentioned that in the experimental charge density maps studied in the case of thiocyanates, the deformation density maps contained a positive region corresponding to the presence of the π-hole.[4–6]

We have studied single crystal structures of four compounds, Fmoc-X-ψ[CH₂NCS] (X = Leu, Ile, Val and Ala; Scheme 1; Fig. S2, ESI†).

Among them, X = Leu crystallizes in a tetragonal space group, $P4_1$ and displays an isomorphous reversible phase transition[11] upon cooling. The phase transition has been characterized by the DSC isotherm, IR spectroscopic measurements and variable temperature cell determination by single crystal X-ray diffraction. Experimental and theoretical charge density analyses have been carried out to elucidate the nature of interactions involving isothiocyanate groups using the data collected at 100 K.

The other three molecules (X = Ile, Val, Ala) crystallize in a monoclinic space group, $P2_1$, and show no phase transitions with temperature. It is interesting to note that the fluorene moiety forms

[a] Solid state and Structural Chemistry Unit, Indian Institute of Science, Bangalore-560012, India. E-mail: ssctng@sscu.iisc.ernet.in; Fax: +91-080-23601310

[b] Peptide Research Laboratory, Department of Studies in Chemistry, Bangalore University, Bangalore-560001, India. E-mail: sureshbabuvommina@rediffmail.com

X=Leu, Ile, Val, Ala

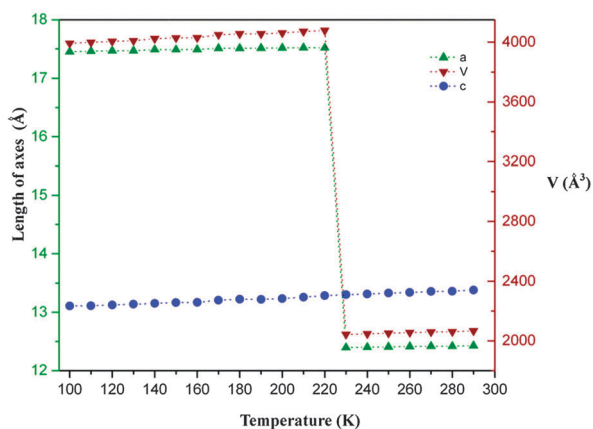**Scheme 1** Structural formula of Fmoc-X-ψ[CH₂NCS].

Fig. 1 Temperature dependence of the unit cell parameters, *a* and *c* axes and the volume (V); sharp jumps in *a* and V are observed at the transition temperature.

edge-to-face C–H⋯π contacts in the case of X = Leu, whereas in the other three structures, face-to-face π⋯π contacts are observed. This ensures that in the case X = Leu, the N═C═S moieties are perpendicular to each other, whereas the N═C═S moieties are parallel to each other in the other three structures (Fig. S3, ESI†).

The reversible isomorphous single crystal to single crystal phase transition in Fmoc-Leu-CH$_2$NCS (room temperature $P4_1$, $Z' = 1$ to low temperature $P4_1$, $Z' = 2$) appears sharply at 230 K. The variable temperature unit cell determination over the temperature range of 290–100 K at intervals of 10 K depicts the evolution of cell parameters, as shown in Fig. 1. The transition at 230 K is very clearly indicated. It is to be noted that during the cooling cycle, at the transition temperature, the *a* axis increases by 41.4% ($\Delta a/a$), which is equivalent to an increase of $\sqrt{2}a$ (diagonal to the original lattice), whereas the *c* axis remains almost unchanged. During the heating cycle, the cell dimension '*a*' reverts to the original value, thus justifying the isomorphous nature of the phase transition. In addition, the doubling of the unit cell volume causes a minor rearrangement in the conformation of the molecules (one rotated by nearly 6° with respect to the other) and reverts to the original $Z' = 1$ structure upon heating beyond 230 K. Fig. 2 represents both these features. The sharp jump in the *a* axis and the volume of the unit cell at the transition temperature is suggestive of a first-order phase transition.‡

The phase transition has also been monitored by FT-IR spectroscopy in the solid state. The room temperature spectrum of Fmoc-Leu-CH$_2$NCS shows strong and very broad absorption with 3 distinct maxima in the range 2050–2200 cm^{-1}, characteristic of an NCS asymmetric stretch, ν_{as}(NCS).[12] Upon initially cooling the compound to 133 K, the spectrum showed almost doubling of peaks in the ν_{as}(NCS) region, thus supporting the phase transition ($Z' = 1$ to $Z' = 2$). Further spectra were recorded in the heating cycle in the temperature range 133–253 K (shown in Fig. 3 in steps of the 10 K min^{-1} heating rate), eventually reaching the room temperature supporting the isomorphous phase transition (Fig. 3).

The approach of the two –NCS groups perpendicular to each other in the crystal structure, thus resulting in the formation of
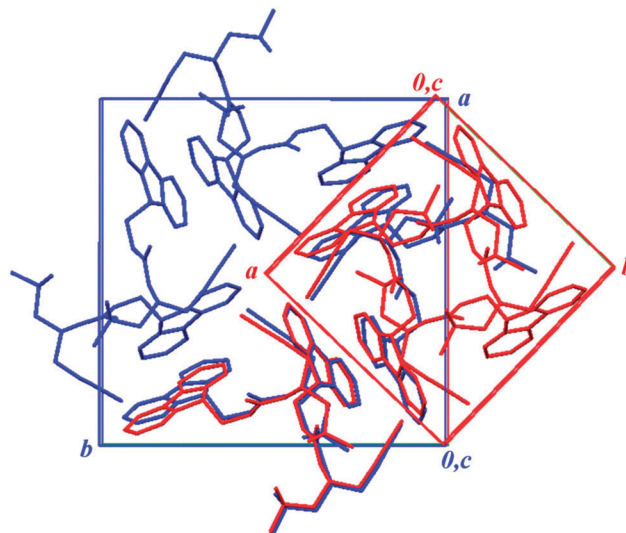

Fig. 2 Overlay diagram of the two forms in a tetragonal $P4_1$ space group, room temp., $Z' = 1$ (red) and low temp. $Z' = 2$ (blue) along the *c* axis.

a N═C═S⋯N═C═S chain along the 4_1 screw axis, prompted us to explore the intermolecular interaction before and after the phase transition. A CSD (v5.35 February 2014) analysis (see ESI†) reveals that this particular interaction mode of NCS groups is sparse in the case of organic molecules. Early database studies[13,14] suggested that electrophiles approach divalent S at approximately 20° from the perpendicular to the plane containing sulfur. It would indicate that the lone pair of electron density associated with the sulfur atom might interact with the electropositive region of the approaching NCS group. In the low temperature $Z' = 2$ structure, the two molecules in the asymmetric unit (MOL1 and MOL2) form similar chains of N═C═S⋯N═C═S contacts with their symmetry equivalent counterparts (Fig. 4).

The N═C═S⋯N═C═S interaction length formed by MOL1 and its symmetry equivalent counterpart gets shorter (S⋯N = 3.296(1) Å; Fig. 4a) compared to the sum of the van der Waals
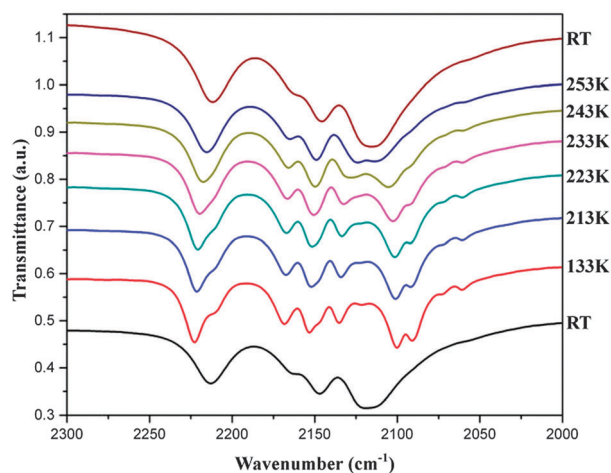

Fig. 3 Changes in variable temperature IR spectra in the region of ν_{as}(NCS) vibration with temperature.
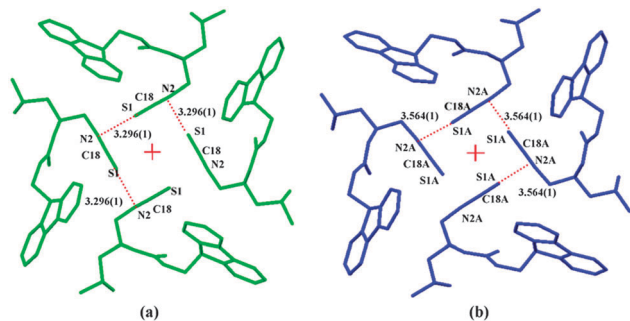
Fig. 4 N=C=S··· N=C=S interactions in (a) MOL1 (green), (b) MOL2 (blue), projection along the c axis. '+' (in red) represents the 4_1 screw axis.
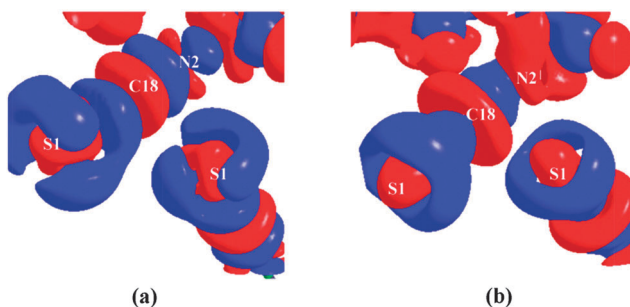

Fig. 5 3D deformation density plots obtained from (a) experimental and (b) theoretical charge density analyses depicting the NCS region in MOL1. Blue and red represent +ve and −ve values, respectively. The $\Delta\rho$ contours are drawn at ± 0.05 e Å^{-3}.

radii of N and S (3.35 Å); we analyzed the experimental charge density data (100 K, see ESI†) to gain insights into this unique interaction.

3D-deformation density ($\Delta\rho = \rho_{\text{multipole}} - \rho_{\text{spherical}}$) maps obtained from experimental and theoretical multipole models depict the presence of both electron-rich (blue) and electron-deficient regions (red) on S as well as along the C=N bond (Fig. 5). Topological analysis given in Table 1, reveals the relative strength of this closed-shell interaction based on the ratio of the local potential energy density to the kinetic energy density ($|V_{\text{bcp}}|/G_{\text{bcp}}$) derived from the $\rho(r)$ and $\nabla^2\rho(r)$ values. Theoretical electron density properties calculated directly from the wave function (the TOPOND program as implemented in CRYSTAL14) are also given in Table 1 for comparison.

Moreover, the short N=C=S···N=C=S interaction in MOL1 needs to be analyzed in terms of its properties. Electrostatic potential

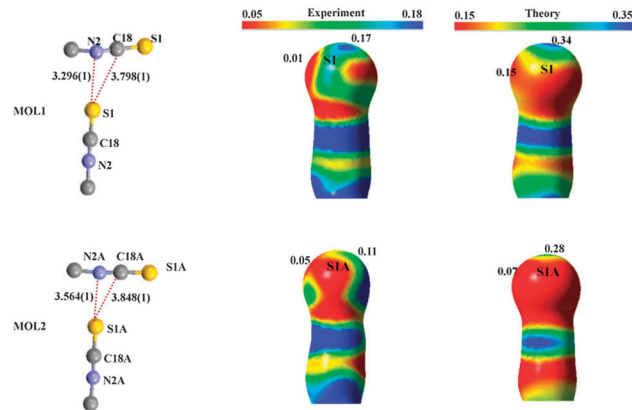Fig. 6 Electrostatic potential mapped on an isodensity surface (0.5 e Å^{-3}), along with the geometrical representation of the C=N=S moiety depicting the characteristics of a σ-hole on S (blue) along the extension of the NCS covalent bond and a π-hole (blue) perpendicular to the CN bond. The first/second row displays the C=N=S moiety for MOL1/MOL2. Blue and red colours represent +ve and −ve regions, respectively.

maps bring out the features vividly as shown in Fig. 6. Electrostatic potential mapped on an isodensity surface (0.5 e Å^{-3}) indicates a σ-hole formation on the S atom along the extension of the covalent bond of the N=C=S group.

The characteristic of the σ-hole on S1 of MOL1 is clearly more prominent (indicated as the blue region on the top surface of S in Fig. 6, first row) compared to the corresponding one on S1A of MOL2 (Fig. 6, second row). In addition, the electrostatic potential values also suggest a π-hole formation on the C=N bond of the neighboring NCS moiety, as described by Politzer's group.[8,15] Fig. 6 displays an appearance of a "blue" band perpendicular to the C=N bond of the neighboring NCS moiety and thus is indicative of a π-hole bonding. The positive σ-holes and π-holes interact cooperatively with the negative sites of the NCS moieties, thereby stabilizing the N=C=S···N=C=S interaction.[15,16]

The occurrence of both "σ-holes" and "π-holes" in the crystal structure of Fmoc-Leu-ψ[CH$_2$NCS] brings out the relevance of weak but highly directional interactions to the fore and provides an unique first time experimental verification.

Notes and references

1 J. Vagner, H. Qu and V. J. Hruby, *Curr. Opin. Chem. Biol.*, 2008, **12**, 292–296.
2 J. S. Nowick, *Org. Biomol. Chem.*, 2006, **4**, 3869–3885.
3 V. V. Sureshbabu, S. A. Naik, H. Hemantha, N. Narendra, U. Das and T. N. Guru Row, *J. Org. Chem.*, 2009, **74**, 5260–5266.
4 P. Munshi, E. Cameron, T. N. G. Row, J. D. Ferrara and T. S. Cameron, *J. Phys. Chem. A*, 2007, **111**, 7888–7897.

Table 1 Topological parameters of the NCS···NCS interaction[a]

S···N	R_{ij} (Å)	$\rho(r)$ (e Å^{-3})	$\nabla^2\rho(r)$ (e Å^{-5})	$|V|/G$	E (kJ mol^{-1})
MOL1 S1···N2	**3.297**	**0.06**	**0.7**	**0.81**	**−3.4**
	3.296	0.06	0.7	0.78	−3.3
	3.294	*0.05*	*0.7*	*0.71*	*−3.0*
MOL2 S1A···N2A	**3.567**	**0.04**	**0.4**	**0.74**	**−3.1**
	3.573	0.04	0.4	0.72	−3.0
	3.575	*0.03*	*0.4*	*0.67*	*−2.8*

[a] For each interaction the first/second/third row represents experimental/theoretical multipole/TOPOND calculated values.

5 J. W. Bats, P. Coppens and A. Kvick, *Acta Crystallogr., Sect. B: Struct. Crystallogr. Cryst. Chem.*, 1977, **33**, 1534–1542.

6 J. W. Bats and P. Coppens, *Acta Crystallogr., Sect. B: Struct. Crystallogr. Cryst. Chem.*, 1977, **33**, 1542–1548.

7 P. Sjoberg and P. Politzer, *J. Phys. Chem.*, 1990, **94**, 3959–3961.

8 J. S. Murray, P. Lane, T. Clark, K. E. Riley and P. Politzer, *J. Mol. Model.*, 2012, **18**, 541–548.

9 X. Q. Yan, X. R. Zhao, H. Wang and W. J. Jin, *J. Phys. Chem. B*, 2014, **118**, 1080–1087.

10 X. Guo, L. Cao, Q. Li, W. Li and J. Cheng, *J. Mol. Model.*, 2014, **20**, 1–6.

11 H.-K. Fun, C. K. Quah, S. R. Jebas and L.-H. Ong, *J. Mol. Struct.*, 2010, **964**, 31–38.

12 P. Majewska, M. Rospenk, B. Czarnik-Matusewicz, A. Kochel, L. Sobczyk and R. Dąbrowski, *Chem. Phys.*, 2007, **340**, 227–236.

13 R. E. Rosenfield Jr, R. Parthasarathy and J. Dunitz, *J. Am. Chem. Soc.*, 1977, **99**, 4860–4862.

14 T. N. G. Row and R. Parthasarathy, *J. Am. Chem. Soc.*, 1981, **103**, 477–479.

15 P. Politzer and J. S. Murray, *ChemPhysChem*, 2013, **14**, 278–294.

16 P. Politzer, J. S. Murray and T. Clark, *Phys. Chem. Chem. Phys.*, 2013, **15**, 11178–11189.